Electron-impact excitation of the 1 $^2S\rightarrow$2 ^2S+2 ^2P levels of atomic hydrogen at 30, 40, 50, 54.4, and 100 eV

M. A. Khakoo,[1] M. Larsen,[1] B. Paolini,[1] X. Guo,[1] I. Bray,[2] A. Stelbovics,[3] I. Kanik,[4] S. Trajmar,[4] and G. K. James[4]

[1]*Department of Physics, California State University, Fullerton, California 92834*
[2]*Flinders University of South Australia, GPO BOX 2100, Adelaide, SA 5001, Australia*
[3]*Center for Atomic, Molecular and Surface Physics, Murdoch University, 6150 Western Australia*
[4]*Jet Propulsion Laboratory, California Institute of Technology, Pasadena, California 91109*

Normalized experimental differential cross sections for the electron impact excitation of the 1 $^2S\rightarrow$2 ^2S +2 ^2P levels of H at 30, 40, 50, 54.4, and 100 eV incident energies are presented. Ratios of scattering intensities of electrons incident on a target mixture of H and He and having excited the H ($n=2$) and He ($n=2$) levels are measured using electron-energy-loss spectroscopy. These intensity ratios are normalized to available, accurate, experimental excitation differential cross sections for He ($n=2$) [except at 54.4 eV, where theoretical He ($n=2$) differential cross sections are used] to obtain relative differential cross sections for electron impact excitation of the H ($n=2$) manifold. The relative H ($n=2$) differential cross sections are placed on an absolute scale by determining the H/He mixture ratio using energy-loss spectra taken at 200 eV and 25° scattering angle, and normalizing to accurate theoretical H ($n=2$) and He ($n=2$) differential cross sections at this energy and scattering angle. Comparisons with available calculations and measurements are made.

I. INTRODUCTION

There exists a long-standing discrepancy between theory and experiment in electron-atom collision physics, regarding differential electron scattering from H at large electron scattering angles; this constitutes the most important problem that needs to be solved in collision physics at the present time [1]. Experimental electron impact excitation data for tests of electron scattering models are available in the form of differential cross sections, coherence and correlation measurements (electron-photon coincidence, polarized-electron scattering asymmetries), and emission cross sections. The reader is referred to the recent reviews of Zecca *et al.* [2] for cross-section measurements and also Crowe *et al.* [3] for electron-photon coincidence studies in H. In the past, electron-photon coincidence measurements [1,4,5] in H and He have provided tests of the existing convergent close-coupling calculations (CCC) of Bray and Stelbovics [6] and Fursa and Bray [7] for electron-H and electron-He scattering. However, while these data provide details of inaccessible cross sections, scattering amplitudes, and phases, the uncertainties in these difficult and time-consuming measurements are typically in the region of 15–20%. More recently, the Maynooth group [8] has carried out electron-photon coincidence measurements of the excitation of the H 1 $^2S\rightarrow$2 ^2P transition at the well-studied incident electron energy (E_0) of 54.4 eV. Their experiment employed a linear ''polarization-correlation'' analysis of the coincident Lyman-α photons, and their results for the reduced Stokes parameter, $\overline{P2}$, show significant differences with the CCC around 90° scattering angle. This is in disagreement with the recent electron-photon ''angular-correlation'' measurements of the Newcastle group [1], which show excellent agreement with the CCC (when converted into the reduced Stokes parameter $\overline{P2}$

[9]). The 1 $^2S\rightarrow$2 ^2P transition of H is easily radiation-trapped even at very low H-beam densities. This effect makes such coincidence measurements in H restricted to low target beam densities, thus making experimental signal rates and accumulated statistics low. At present, there are also some uncertainties about the reliability of the CCC for providing highly accurate scattering amplitudes for electron-H scattering as it does for electron-He scattering. A popular argument which supports this is that H has considerably higher dipole polarizability (0.67×10^{-30} m^3) than He (0.2×10^{-30} m^3) [2,10]. This long-range polarization potential increases the number of partial waves required for the convergence of scattering models and could thus give additional difficulties for the CCC in H as compared to He. This query has not been clarified experimentally for H differential cross sections (DCS's), where the situation for e^- + H scattering is unsatisfactory. At $E_0=54.4$ eV, some discrepancies exist between the H ($n=2$) DCS's of Williams and Willis [11] and the CCC [6]. There is some concern at $E_0=54.4$ eV when one compares the William and Willis DCS's to those of the CCC here because the disagreements between the CCC and Williams and Willis' data exceed 25% (four standard deviations) in places. At $E_0=100$ eV above $\theta>80°$, the H ($n=2$) DCS's of Williams and Willis exceed the CCC by greater than a factor of 2. At this E_0 there also exist DCS's taken by the John Hopkins group [12] using the method of mixtures (a supersonic H source was seeded with He as a calibration standard) for the electron impact excitation of the H ($n=2$) manifold. These DCS's show severe disagreements with the CCC at θ above 90°, by a factor of greater than 4. These disagreements are possibly due not only to the significant experimental problems in working with (dissociated) atomic hydrogen beams, but also in the systematic uncertainties in such experiments which dominate in the pro-

cess of normalizing inelastic scattering intensities to elastic scattering DCS's in these experiments. Conventionally, elastic scattering cross sections in such $e^- + H$ collision experiments are obtained by the discharge modulated-beam method [13], where it is assumed that the concentration of excited (metastable) state H species is negligible. Because of this, the number density of atoms/molecules in discharge on/off conditions in the target region is related by a simple formula containing the dissociation fraction, the masses of the species, and the temperature for the discharge on/off conditions. However, the elastic electron scattering signal can be plagued by background from primary beam electrons reflecting (elastically) from surfaces around the collision region, making the determination of the elastic scattering signal prone to systematic errors. Further, beams of H are generated from dissociation of H_2 and thus always contain an H_2 component. This H_2 fraction has to be precisely known in order to determine elastic scattering from H alone. The determination of H:H_2 ratios in the target beams used in these experiments makes them difficult in order to be accurate. That such problems (outlined above) are difficult to work around can be gauged from the disagreements between existing $e^- + H$ elastic scattering DCS measurements [13,14].

The experimental method of gas mixtures does not have the problems encountered in the conventional modulated-beam method. In this method the H beam is mixed with an inert gas whose inelastic cross sections are accurately known (i.e., a standard target). By monitoring the energy-loss features of H and the standard target, it is possible to measure inelastic cross sections where one monitors only inelastically scattered electrons. By only monitoring inelastically scattered electrons, one can separate the $e^- + H$ from the $e^- + H_2$ inelastic features (or for that matter H/H_2 and the standard gas target) using electron-energy-loss spectroscopy. This mode of operation also reduces the pernicious effect of background electrons from the collision region. This also provides an alternative method for obtaining accurate inelastic DCS's for electron scattering from H. As mentioned, this method has been employed by the John Hopkins University group [12]. However, their results also show severe disagreement with those of the CCC and Williams and Willis [11]. On reexamination, we realized that this method should work well provided the gases were well-mixed and effusively introduced into the target region (equal mean free paths). Additional observations that background electron scattering signals in inelastic scattering channels were significantly lower than corresponding backgrounds in the elastic scattering channel encouraged us to make a new attempt at measuring H ($n=2$) DCS's using the method of mixtures.

In this paper, we present measurements of normalized DCS's for excitation of the $n=2$ manifold of H via the method of mixtures. Here we use existing accurate electron-He inelastic experimental DCS's as our calibration standard for relative DCS's and accurate and consistent $e^- + H$ and $e^- + He$ theoretical DCS's as our absolute calibration standards. This paper is also a full version of a letter published earlier [15].

II. EXPERIMENTAL APPARATUS

Our apparatus has been discussed previously (see Ref. [16] and the references therein), so only a brief summary will be given here. The atomic beam is generated by a capillary needle, and made to cross a monochromatic beam of electrons produced by a single-hemispheric electron gun of an electrostatic electron spectrometer in a conventional crossed beam-beam configuration. This experiment was previously used for electron-photon coincidence studies [16], in which to reduce the detection of metastable He atoms by an open VUV photon detector the gas jet was angled at 45° to the scattering plane (away from the VUV detector); it was left in this position for this experiment. Scattered electrons were energy-analyzed by the spectrometer's electrostatic analyzer as a function of energy loss ΔE and scattering angle θ. The spectrometer performed with typical currents of ≈ 0.2–0.3 μA and with an energy resolution of 170–200 meV [full width at half-maximum (FWHM)]. This spectrometer is stable over very long periods (> 1 year). The unit is baked at ≈ 110–120 °C to maintain stability against oil contamination. It is enclosed in a double mu-metal shield which reduced the Earth's magnetic field below 5 mG. Its data acquisition and control system is computerized (angle settings, multichannel sweep, pressure monitoring, etc.), thus allowing for the continuous (overnight) and hence efficient collection of data. The angular resolution of the spectrometer is 2.5° (FWHM) and the location of the angles is within ± 1.0°. Finally, its contact potential was measured using the elastic scattering 2 ^2S resonance in He at 19.366 ± 0.005 eV [17] and was found to be in the range of 0.65–0.8 eV. Our incident energy is therefore accurate to approximately ± 0.1 eV.

For our gas source, we have used a recently developed, intense, and very stable H source that is detailed in a recent publication [18]. The H source is an extended cavity microwave discharge of 99.999% purity H_2, operating at 2450 MHz, which utilizes Teflon tubing to conduct the atoms to the collision region, where the tubing is terminated by a outside-silvered glass needle (0.5-mm internal diameter), but inside-coated with Teflon using a solution of Teflon FEP, provided to us by the Dupont company [18]. This source operates with a high H/H_2 dissociation fraction of 85% (under presently optimum conditions). In this work typical dissociation fractions ranged from 75% to 80%. This fraction is stable over periods exceeding a month. Typically, a mixture ranging from a 0.5:0.5 to 0.6:0.4 (by pressure) of H_2 to He was used, and was introduced into the discharge tube through separate precision leak valves. At the working pressure (typically 0.5 Torr of H_2+He), the experimental background pressure increased from a base of 8×10^{-8} to 1.6 $\times 10^{-6}$ Torr. The discharge was allowed to stabilize overnight and was checked for stability by monitoring electron energy-loss spectra with the electron spectrometer. The pressure fluctuation of the discharge during the entire experiment (for H and He together) did not exceed 2% as measured upstream of the discharge using a temperature-stabilized capacitance manometer. We noticed that during the course of data measurements, the discharge (characteristically bright red) would suddenly turn pink and result in a complete loss
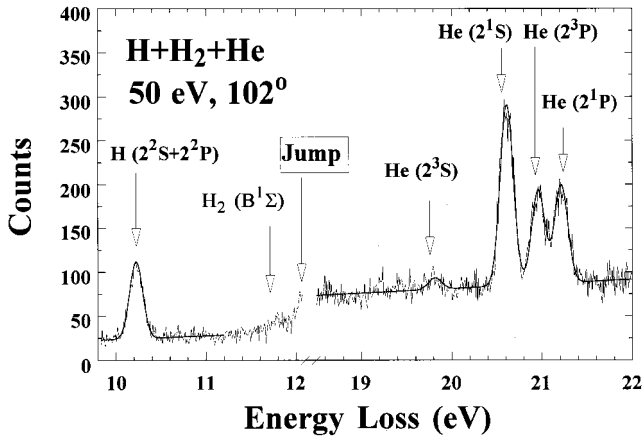
FIG. 1. Typical electron-energy-loss spectrum of He+H+H$_2$ taken at $E_0 = 50$ eV and $\theta = 102°$ from this experiment. Pertinent energy-loss features are labeled and the fits (heavy solid lines) to unfold the data are shown. See text for details.

of H. This loss of H would last from 30 min to 1 h. When the source returned to its bright red color, the dissociation reverted quickly (within a few minutes) to its normal value. The reason for this instability is not understood, but it is correlated with the presence of He in the discharge tube. It could be possibly due to a change in the surface of the discharge induced by the He for a short period of time due to metastable degradation of the surface or some other chemical reaction of the He with the discharge glass wall. In any case, data taken under these conditions were rejected. On resum-

ing normal operation, we were able to reproduce spectra very accurately and easily to within 3% uncertainty across the spectrum of H and He.

III. EXPERIMENTAL METHOD

Our measurements were made in two stages. The first stage involved the determination of relative DCS's for excitation of the H ($n=2$) manifold. The second stage involved the normalization of the relative DCS's to absolute values.

A. Relative DCS measurements

First, data which were comprised of electron-energy-loss spectra covering (simultaneously) the energy-loss range of 9.7–12.2 eV [H ($n=2$) features] and 19.5–22.0 eV [He ($n=2$) features] were taken in continuous scans and scattering angles in the range of 10°–127° in 5° intervals. A typical spectrum is shown in Fig. 1. Spectra were taken in a quasi-random sequence, and angles were repeated in most cases at least in triplicate to check reproducibility or to improve statistics. Such spectra were taken at the E_0 values of 30, 40, 50, 54.4, and 100 eV. The ratio $R_{H/He}$ of the scattering intensities for the energy-loss feature for the $1\ ^2S \rightarrow 2\ ^2S + 2\ ^2P$ levels of atomic hydrogen and the summed $1\ ^1S \rightarrow 2\ ^1S + 2\ ^3P + 2\ ^1P$ levels of He was determined from each energy-loss spectrum (see Fig. 1). This ratio is related to the respective DCS's $(d\sigma/d\Omega)$/of the H and He inelastic features by

$$R_{H/He}(E_0,\theta) = \frac{T(E_0,\Delta E_H)I_0 n_H (l\Delta\Omega_{eff}) \dfrac{d\sigma}{d\Omega}[H(2\ ^2S + 2\ ^2P)]}{T(E_0,\Delta E_{He})I_0 n_{He}(l\Delta\Omega_{eff})\dfrac{d\sigma}{d\Omega}[He(2\ ^1S + 2\ ^3P + 2\ ^1P)]}, \tag{1}$$

where I_0 is the incident electron current, n_H and n_{He} are the respective average number densities for H and He in the collision region, and $(l\Delta\Omega_{eff})$ is the "effective" overlap of the electron beam through the gas beam (l) and the spectrometer analyzer acceptance view cone, $\Delta\Omega$. $(d\sigma/d\Omega)[H(2\ ^2S + 2\ ^2P)]$ and $(d\sigma/d\Omega)[He(2\ ^1S + 2\ ^3P + 2\ ^1P)]$ are the respective DCS's for excitation of the above-mentioned H and He levels of interest from their respective ground states. $T(E_0,\Delta E)$ is the transmission efficiency of the electron detector for the different energy-loss electrons for the excitation of H ($=\Delta E_H$) and He ($=\Delta E_{He}$), relative to the elastic ($\Delta E=0$) energy loss.

The effect utilized in the method of mixtures is that the term ($l\Delta\Omega_{eff}$) in Eq. (1) is nearly identical for both gases; since the gases are well-mixed, the collisional mean free path of both species is the same. The complete gas mixing is ensured in the configuration here since the mean free path of the gases ($\approx 10^{-4}$ m) is much shorter than the length of the

gas-handling system (≈ 1 m). The ratio $R_{H/He}$ in Eq. (1) then becomes directly proportional to the DCS ratio of the two gases, which are related to their respective scattering intensities by the ratio of n_H and n_{He} and $T(E_0,\Delta E_H)$ and $T(E_0,\Delta E_{He})$. Thus, relative DCS's for the unknown gas (H in our case) may be determined from relative DCS's of the calibration gas (He in this experiment) using Eq. (1).

The proper implementation of the method of mixtures depends on several factors which we now list, together with their handling in our experiment.

(i) The electron-energy-loss spectra of the mixture do not interfere with each other, so that pertinent, individual spectral features can be isolated. This is clearly the case for the features in question here (Fig. 1) where the H ($n=2$) features are sited on a smooth H$_2$ $b\ ^3\Sigma_u^+$ continuum and the He ($n=2$) features lie on a flat H/H$_2$ ionization continuum. Both H and He ($n=2$) features can consequently be separated

easily from other background features. In this work, the intensities of the relevant energy-loss features were determined by using a spectrum-fitting code which has been developed in our laboratory [19]. The instrumental profile used in this code was that of the H ($n=2$) energy-loss feature, after a linear background was subtracted from it. This instrumental profile was used to fit the He features located on a smooth H/H_2 ionization continuum. The continuum could be adequately described by a polynomial of up to second order, although in most cases (especially at larger E_0 values) a first-order polynomial sufficed.

(ii) The flow of constituent atoms in the mixture is stable, which implies a stable H source, i.e., that the dissociation fraction of H in the source is constant. This is also the case for the present experiment, where runs of several days could be made over essentially identical flow conditions with an estimated 2% stability in the mixture, based on observed ratios as well as pressure stability of the discharge. To ensure stable operation, only metal tubes (copper mainly) or Teflon tubes (inside the vacuum chamber) were used to handle the gas. The gases were regulated into the discharge using double-stage gas regulators with all metal diaphragms and bakeable precision leak valves [20].

(iii) The transmission of the electron analyzer remained constant during the course of the experiment. This was ensured in this experiment by *not* retuning the electron analyzer during the course of the experiment, and keeping the system heated (see Sec. II) to stabilize the lens' surfaces. The results of these actions enabled us to successfully reproduce cross-section ratios.

(iv) Electron scattering from background gas in the vacuum tank can be accurately measured or is negligible. This is especially a problem with H since it only partially recombines with the walls of the vacuum tank [21] and is thus present in the background. The inelastic, background electron scattering signal from He was measured for a range of θ from 5° to 120°, at the different E_0 values. We observed that it maximized to approximately 10% at small θ (depending on the E_0 value, i.e., $\theta < 20°$ at $E_0 = 30$ eV and $\theta < 5°$ at $E_0 = 100$ eV) and reduced to less than 2% at large θ. Not knowing the exact contribution of H, we have conservatively added the full uncertainty in the He background to our results, assuming on the outside limit that the background errors are the same for both gases.

(v) Accurate relative DCS's need to be available for the standardizing gas. The DCS's for the summed $1\,^1S \rightarrow 2\,^1S + 2\,^3P + 2\,^1P$ transitions in He were taken at $E_0 = 30$, 40, and 50 eV from a recent experiment of Roder *et al.* [22] ($\pm 5\%$ relative), which is in excellent agreement (within $\pm 5\%$) with the very early measurements of Hall *et al.* [23] (uncertainties of $\pm 5\%$ relative and $\pm 15\%$ absolute; see, e.g., Fig. 2) and in reasonable agreement (within $\pm 10\%$ relative) with the measurements of the JPL-LANL group [24,25]. However, the Roder *et al.* measurements constitute separate relative measurements for the $1\,^1S \rightarrow 2\,^1S$, $2\,^3P$, $2\,^1P$ transitions. Therefore the ratios of the $2\,^1S:2\,^3P:2\,^1P$ in this data set were established using the $2\,^1S:2\,^3P:2\,^1P$ ratios from the DCS's of Hall *et al.* [23] (interpolated by a polynomial least-squares fit where necessary, and averaged over scattering angles of 20° to 120°). At $E_0 = 100$ eV, we used the DCS's for the summed $1\,^1S \rightarrow 2\,^1S + 2\,^3P + 2\,^1P$ transitions in He of the JPL-LANL group [24,25], which are the only available experimental DCS's. We notice the disagreement between the CCC [7] and the experimental He DCS's at large scattering angles. This will be discussed in more detail in Sec. V A concerning the He $1\,^1S \rightarrow 2\,^1S + 2\,^3P + 2\,^1P$ standard. At $E_0 = 54.4$ eV we employed the CCC He DCS's of Fursa and Bray [7] for our calibration standard, because there exist no inelastic experimental DCS's available for He at $E_0 = 54.4$ eV to enable us to normalize our $R_{H/He}$ values at this energy

B. Normalized DCS measurements

In the next stage our relative H ($n=2$) DCS's were normalized to the mean theoretical values for the H ($n=2$) DCS calculated from the distorted-wave Born approximation (DWBA) [26] and the CCC [6] at 200 eV and 25°. These E_0 and θ were chosen because whereas these models are different approaches, they both agree to better than 2% for $\theta \leqslant 40°$. This normalization was achieved by taking similar energy-loss spectra as in Fig. 1 at 200 eV, 25° and the impact energy of interest (in this case 30, 40, 50, 54.4, and 100 eV) at 25° for the same conditions in the H discharge source. It can be readily shown, using parameters already defined in Eq. (1), that

$$\frac{d\sigma_H(E_0, 25°)}{d\Omega} = \frac{[d\sigma_{He}(E_0,25°)/d\Omega][d\sigma_H(200\,\text{eV},25°)/d\Omega]T_{He}(E_0)T_H(200\,\text{eV})l_H^s(E_0)l_{He}^s(200\,\text{eV})}{[d\sigma_{He}(200\,\text{eV},25°)/d\Omega]T_H(E_0)T_{He}(200\,\text{eV})l_{He}^s(E_0)l_H^s(200\,\text{eV})}, \tag{2}$$

i.e., the aim of the normalization is to determine the ratio n_H and n_{He} in Eq. (1). The additional factors in Eq. (2) which must be determined are $T_H(E_0)$, $T_{He}(E_0)$, $T_{He}(200\,\text{eV})$, and $T_H(200\,\text{eV})$. These are the transmission characteristics of the analyzer; here we make the assumption that $T(E_0, \Delta E)$

$\cong T(E_R)$, where E_R ($= E_0 - \Delta E$) is the residual energy of the scattered electron, i.e., the detection efficiency of electrons by the analyzer is primarily dependent on the electron residual energy. This is reasonable, because Eq. (2) uses ratios of intensities at the same E_0 value and thus suppresses the
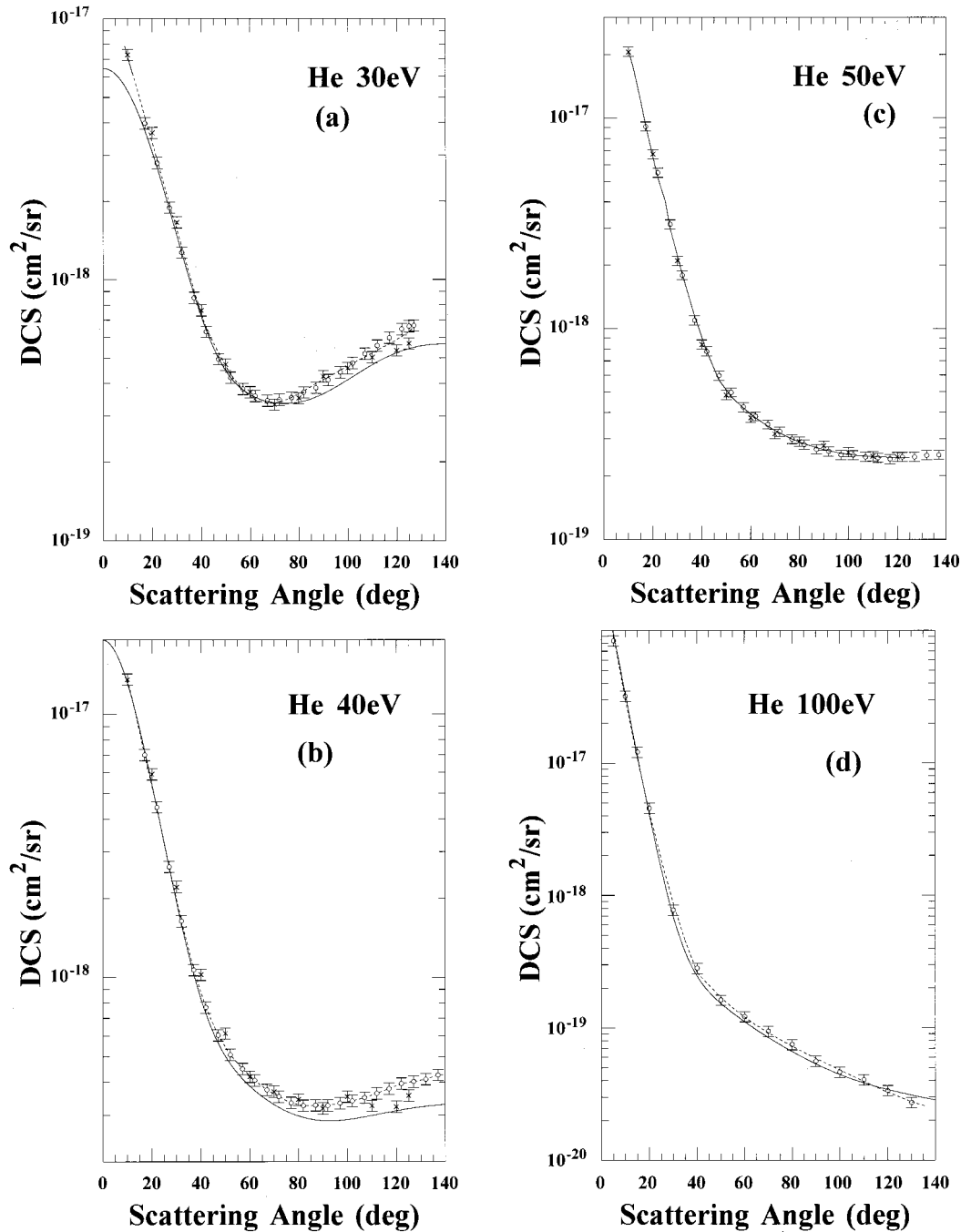
FIG. 2. (a)–(d) Experimental relative DCS's at various E_0 values for electron impact excitation of the He $1\,^1S \rightarrow 2\,^1S + 2\,^3P + 2\,^1P$ levels. The He DCS's used as a calibration standard at 30, 40, and 50 eV were obtained from a smooth polynomial fit ($\cdots$) to DCS's of Refs. [22] ($\bigcirc$) and [23] ($\times$) combined (with 5% relative error bars shown), and at $E_0 = 100$ eV from ($\bigcirc$) Refs. [24] and [25]. The CCC of Ref. [7] (——) is also shown. See text for discussion.

influence of the incident electron beam profile on the measurement of $d\sigma_H(E_0,25°)/d\Omega$. This suppression is valid if the analyzer is not retuned and the electron beam is stable during these measurements and θ is held fixed, conditions that are held in our measurements. The $T(E_R)$ for various E_R was made with He alone by measuring elastic and inelastic energy-loss spectra (for the summed He $2\,^1S + 2\,^3P + 2\,^1P$ transitions) at $E_0 = 200, 100, 75, 60, 50,$ and 40 eV at 25° as well as $E_0 = 30$ eV at 90°. These measurements were taken

with gas through the capillary tube (signal+background), and the same gas routed into the vacuum tank via a side leak (background). Theoretical elastic and inelastic He DCS's [7] at $E_0 = 100, 75, 60, 50,$ and 40 eV and $\theta = 25°$ and experimental elastic [27] and inelastic [23] He DCS's at $E_0 = 30$ eV and $\theta = 90°$ were used. This choice is made since we have observed that (during the course of this work) the summed He $2\,^1S + 2\,^3P + 2\,^1P$ experimental DCS's available show excellent agreement with the CCC at small θ
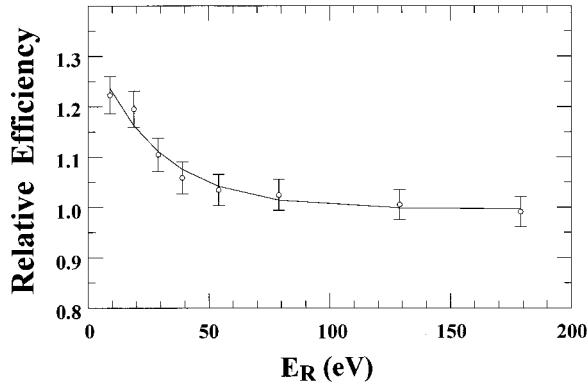
FIG. 3. Relative electron detection efficiency $T(E_R)$ of the analyzer determined in absolute DCS normalization experiments. The line is an exponential fit used to interpolate the values of $T(E_R)$ in this work.

$<50°$, but deviate from the CCC at large angles. We show this transmission function in Fig. 3. The resulting errors from this normalization procedure are 3% for the transmission function and an additional $<2\%$ for the statistical errors compounded with cross sections used for He ($2 \, {}^1S + 2 \, {}^3P + 2 \, {}^1P$) and H ($n=2$). The reproducibility of the measurement of the H DCS's at the required E_0 values was in the region of $\pm 5\%$, which demonstrates the stability of our apparatus.

IV. RESULTS

The $R_{H/He}$ and DCS values from our measurements are shown in Tables I and II, respectively. The sources of experimental errors and their average values are itemized in Table III. These results are plotted and compared to other measurements in Figs. 4 and 5. Error bars are quoted to one standard deviation, i.e., to within a 68% confidence limit.

V. COMPARISON WITH EXPERIMENT AND THEORY

A. Ratios

In Figs. 4(a)–4(e) we show our measured $R_{H/He}$ taken from our electron-energy-loss spectra compared to the theoretical $R_{H/He}$ of Ref. [6] and [7] as well as the experimental values of Ref. [12] at $E_0 = 100$ eV. The theory is scaled up to our results at small θ. This scaling at small θ stems from the observation that the He DCS's from the CCC deviate from the experimental values at larger scattering angles as shown in Fig. 2. This effect will be discussed later on in this paper. In Fig. 4, general agreement of $R_{H/He}$ between theory and experiment is good, yet we observe significant large-angle deviation expected. At $E_0 = 30$, 40, 50, and 54.4 eV we observe that our $R_{H/He}$ values tend to fall 20–30% below that of the CCC. However, at 100 eV, agreement is excellent, indicating a problem with the theoretical $R_{H/He}$ values at low energies. This result is addressed in the sections following

TABLE I. $R_{H/He}$ values determined from the present experiment with associated errors.

Angle (deg)	30 eV	Error	Angle (deg)	40 eV	Error	Angle (deg)	50 eV	Error	Angle (deg)	54.4 eV	Error	Angle (deg)	100 eV	Error
12	7.91	0.90	12	2.87	0.28	10	3.62	0.30	10	2.49	0.23	5	1.88	0.16
17	5.25	0.51	17	1.91	0.16	12	2.90	0.14	15	1.60	0.12	10	1.05	0.07
22	3.92	0.35	22	1.31	0.10	15	2.67	0.09	20	1.18	0.07	15	0.745	0.039
27	2.57	0.17	27	0.994	0.062	17	2.11	0.07	25	0.837	0.048	20	0.555	0.026
32	2.17	0.12	32	0.783	0.045	20	1.77	0.05	30	0.670	0.037	25	0.434	0.023
37	1.74	0.09	37	0.696	0.037	22	1.45	0.04	35	0.575	0.029	30	0.390	0.019
42	1.54	0.09	42	0.643	0.031	25	1.29	0.04	40	0.558	0.029	35	0.411	0.020
47	1.49	0.08	47	0.588	0.029	27	1.07	0.05	45	0.460	0.021	40	0.379	0.019
52	1.44	0.07	52	0.549	0.027	32	0.859	0.038	50	0.440	0.022	45	0.343	0.016
57	1.45	0.08	57	0.552	0.024	37	0.739	0.034	55	0.405	0.019	50	0.322	0.015
62	1.32	0.07	62	0.502	0.026	42	0.718	0.034	60	0.358	0.016	55	0.246	0.010
67	1.29	0.07	67	0.461	0.022	47	0.669	0.025	65	0.345	0.018	60	0.232	0.011
72	1.15	0.06	72	0.436	0.023	52	0.650	0.021	70	0.342	0.016	65	0.236	0.011
77	0.939	0.044	77	0.409	0.018	57	0.632	0.021	75	0.295	0.014	70	0.192	0.010
82	0.770	0.045	82	0.362	0.017	62	0.488	0.016	80	0.240	0.011	75	0.165	0.008
87	0.654	0.037	87	0.308	0.017	67	0.465	0.015	85	0.202	0.011	80	0.158	0.008
92	0.523	0.029	92	0.246	0.012	72	0.457	0.014	90	0.199	0.012	85	0.178	0.009
97	0.439	0.019	97	0.232	0.011	77	0.382	0.015	95	0.172	0.009	90	0.141	0.007
102	0.388	0.025	102	0.185	0.009	82	0.328	0.012	100	0.172	0.008	95	0.194	0.011
107	0.321	0.015	107	0.169	0.009	87	0.330	0.012	105	0.133	0.006	100	0.121	0.006
112	0.298	0.013	112	0.154	0.009	92	0.276	0.011	110	0.144	0.008	105	0.134	0.007
117	0.260	0.012	117	0.132	0.007	97	0.256	0.012	115	0.122	0.006	110	0.131	0.007
122	0.228	0.015	122	0.108	0.006	102	0.221	0.010	120	0.132	0.009	115	0.112	0.007
125	0.236	0.014	127	0.109	0.007	107	0.182	0.007	125	0.109	0.007	120	0.119	0.008
						112	0.186	0.005				125	0.114	0.006
						117	0.150	0.007						
						122	0.156	0.008						
						125	0.149	0.007						

TABLE II. Present determinations of the electron impact DCS's for excitation of the $H(1\,^2S)\rightarrow H(2\,^2S+2\,^2P)$ transitions. Numbers in brackets denote powers of 10.

Angle (deg)	30 eV	Error	Angle (deg)	40 eV	Error	Angle (deg)	50 eV	Error	Angle (deg)	54.4 eV	Error	Angle (deg)	100 eV	Error
12	1.35 [−16]	2.3 [−17]	12	1.26 [−16]	2.0 [−17]	10	1.76 [−16]	3.0 [−17]	10	1.78 [−16]	2.2 [−17]	5	5.56 [−16]	8.6 [−17]
17	6.08 [−17]	9.9 [−18]	17	5.18 [−17]	8.1 [−18]	12	1.16 [−16]	1.8 [−17]	15	6.10 [−17]	6.7 [−18]	10	1.19 [−16]	1.7 [−17]
22	3.11 [−17]	4.9 [−18]	22	2.25 [−17]	3.4 [−18]	15	7.44 [−17]	1.1 [−17]	20	2.30 [−17]	2.3 [−18]	15	3.19 [−17]	4.4 [−18]
25	2.07 [−17]	2.5 [−18]	25	1.51 [−17]	1.8 [−18]	17	4.52 [−17]	6.9 [−18]	25	8.39 [−18]	6.6 [−19]	20	8.94 [−18]	1.2 [−18]
27	1.37 [−17]	2.0 [−18]	27	1.01 [−17]	1.5 [−18]	20	2.68 [−17]	4.1 [−18]	30	3.59 [−18]	3.5 [−19]	25	2.60 [−18]	3.6 [−19]
32	7.99 [−18]	1.1 [−18]	32	4.97 [−18]	7.1 [−19]	22	1.75 [−17]	2.7 [−18]	35	1.77 [−18]	1.7 [−19]	30	1.07 [−18]	1.5 [−19]
37	4.35 [−18]	6.1 [−19]	37	2.87 [−18]	4.0 [−19]	25	1.12 [−17]	1.6 [−18]	40	1.09 [−18]	1.0 [−19]	35	6.51 [−19]	8.9 [−20]
42	2.75 [−18]	3.9 [−19]	42	1.91 [−18]	2.6 [−19]	27	7.44 [−18]	1.2 [−18]	45	6.51 [−19]	5.9 [−20]	40	3.78 [−19]	5.2 [−20]
47	2.16 [−18]	3.0 [−19]	47	1.37 [−18]	1.9 [−19]	32	3.60 [−18]	5.6 [−19]	50	5.02 [−19]	4.7 [−20]	45	2.42 [−19]	3.3 [−20]
52	1.71 [−18]	2.4 [−19]	52	1.08 [−18]	1.5 [−19]	37	1.97 [−18]	3.1 [−19]	55	4.02 [−19]	3.7 [−20]	50	1.84 [−19]	2.5 [−20]
57	1.51 [−18]	2.1 [−19]	57	9.60 [−19]	1.3 [−19]	42	1.29 [−18]	2.0 [−19]	60	3.21 [−19]	2.9 [−20]	55	1.21 [−19]	1.6 [−20]
62	1.26 [−18]	1.8 [−19]	62	7.90 [−19]	1.1 [−19]	47	8.82 [−19]	1.4 [−19]	65	2.84 [−19]	2.7 [−20]	60	9.98 [−20]	1.4 [−20]
67	1.19 [−18]	1.7 [−19]	67	6.67 [−19]	9.2 [−20]	52	7.15 [−19]	1.1 [−19]	70	2.59 [−19]	2.4 [−20]	65	8.97 [−20]	1.2 [−20]
72	1.07 [−18]	1.5 [−19]	72	5.96 [−19]	8.4 [−20]	57	6.13 [−19]	9.4 [−20]	75	2.05 [−19]	1.9 [−20]	70	6.39 [−20]	8.9 [−21]
77	9.14 [−19]	1.3 [−19]	77	5.29 [−19]	7.3 [−20]	62	4.26 [−19]	6.6 [−20]	75	1.54 [−19]	1.4 [−20]	75	4.89 [−20]	6.8 [−21]
82	7.92 [−19]	1.1 [−19]	82	4.57 [−19]	6.3 [−20]	67	3.70 [−19]	5.7 [−20]	85	1.21 [−19]	1.1 [−20]	80	4.18 [−20]	5.8 [−21]
87	7.20 [−19]	1.0 [−19]	87	3.90 [−19]	5.5 [−20]	72	3.38 [−19]	5.2 [−20]	90	1.13 [−19]	1.1 [−20]	85	4.06 [−20]	5.6 [−21]
92	6.09 [−19]	8.6 [−20]	92	3.12 [−19]	4.3 [−20]	77	2.65 [−19]	4.1 [−20]	95	9.37 [−20]	8.8 [−21]	90	2.78 [−20]	3.8 [−21]
97	5.44 [−19]	7.5 [−20]	97	2.99 [−19]	4.1 [−20]	82	2.16 [−19]	3.3 [−20]	100	9.09 [−20]	8.4 [−21]	95	3.48 [−20]	4.9 [−21]
102	5.10 [−19]	7.4 [−20]	102	2.44 [−19]	3.4 [−20]	87	2.08 [−19]	3.2 [−20]	105	6.93 [−20]	6.4 [−21]	100	1.98 [−20]	2.8 [−21]
107	4.45 [−19]	6.2 [−20]	107	2.29 [−19]	3.2 [−20]	92	1.68 [−19]	2.6 [−20]	110	7.40 [−20]	7.0 [−21]	105	2.07 [−20]	2.9 [−21]
112	4.40 [−19]	6.0 [−20]	112	2.17 [−19]	3.1 [−20]	97	1.52 [−19]	2.4 [−20]	115	6.18 [−20]	5.7 [−21]	110	1.87 [−20]	2.6 [−21]
117	4.06 [−19]	5.6 [−20]	117	1.93 [−19]	2.7 [−20]	102	1.29 [−19]	2.0 [−20]	120	6.57 [−20]	6.7 [−21]	115	1.42 [−20]	2.0 [−21]
122	3.79 [−19]	5.5 [−20]	122	1.65 [−19]	2.3 [−20]	107	1.04 [−19]	1.6 [−20]	125	5.35 [−20]	5.5 [−21]	120	1.40 [−20]	2.0 [−21]
125	4.10 [−19]	5.9 [−20]	127	1.69 [−19]	2.4 [−20]	112	1.06 [−19]	1.6 [−20]				125	1.21 [−20]	1.7 [−21]
						117	8.52 [−20]	1.3 [−20]						
						122	8.87 [−20]	1.4 [−20]						
						125	8.48 [−20]	1.3 [−20]						

this one. Comparison at $E_0 = 100$ eV with the $R_{H/He}$ values of Doering and Vaughan [12] (which have larger error bars, $\pm 15\%$, and show considerable scatter) shows that their measurements are in reasonable agreement with ours at small angles. However, their $R_{H/He}$ at $\theta = 90°$ and $120°$ are over an order of magnitude larger than the present measurements.

B. DCS's

In Figs. 5(a)–5(e), we plot our DCS's in comparison to the CCC [6] and the distorted-wave (DW) calculations of Madison [26]. At $E_0 = 100$ eV there also exists a 17-state close-coupling calculation of Wang *et al.* [28], which is in excellent agreement with the CCC at less than 2% across the complete range of θ and has thus been omitted for the sake of duplicity and clarity in the plots.

At $E_0 = 30$ eV [Fig. 5(a)], we observe excellent agreement with the CCC as demonstrated by a (reduced-chi-squared) χ_ν^2 of 0.34. The reason for this "overestimation" is due to the fact that the normalization shifts the entire relative curve ($\pm 9.5\%$), and so each data point is not independently $\pm 15.5\%$ in uncertainty. Comparison with the DWBA [28] shows that the DWBA is clearly in disagreement with the present results by as much as 60% at large angles, i.e., well outside of the error bars. However, the DWBA is an intermediate-to high-energy E_0 theory, and is not expected to be reliable at this E_0. In Figs. 5(b) and 5(c) the agreement with the CCC remains excellent, and there is better agree-

TABLE III. Summary of % errors encountered in this experiment (errors are 1 standard deviation, or 68% confidence limits).

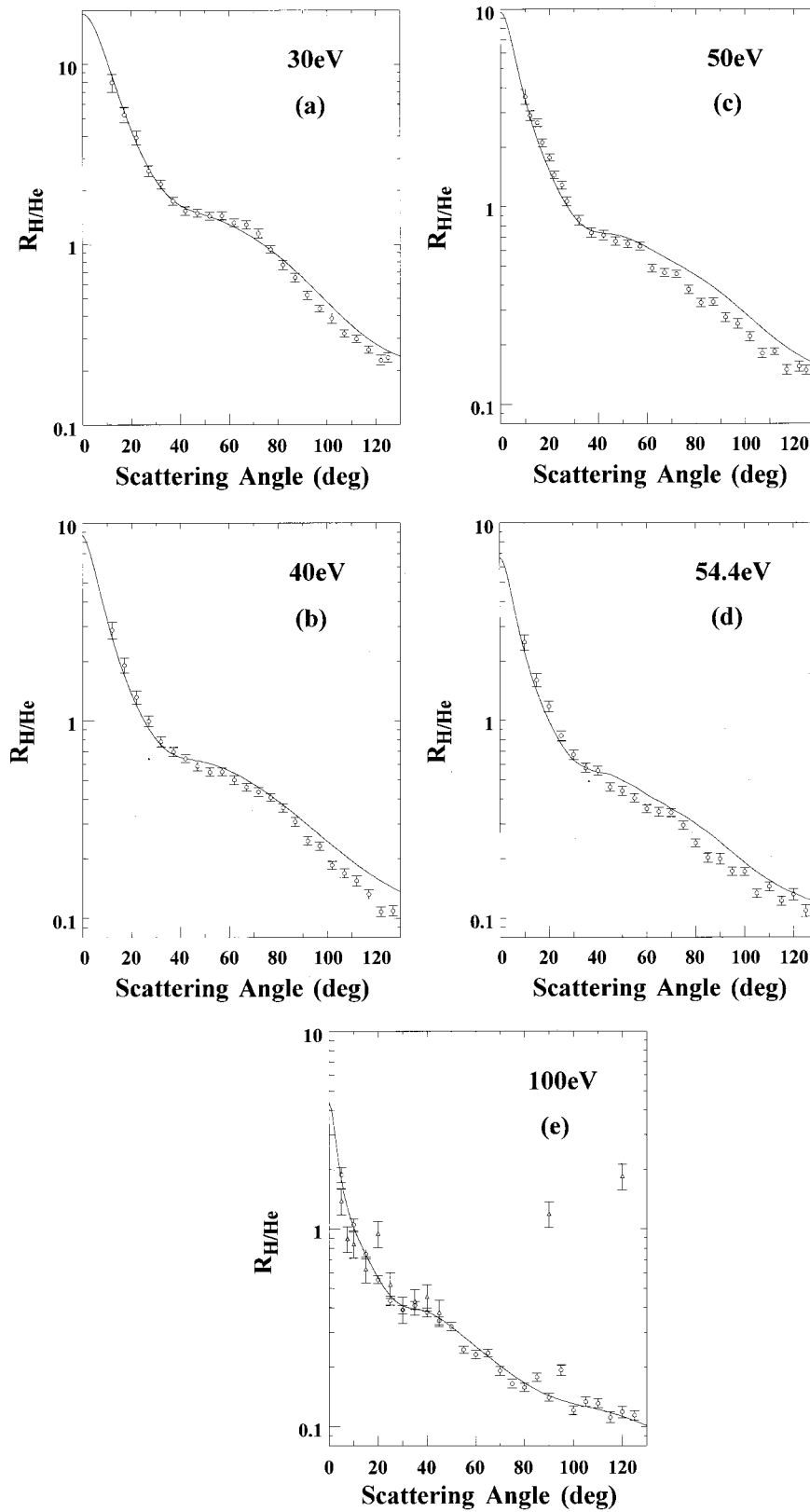| E_0 (eV)	Statistical and fitting	Gas beam stability	Background fraction	He standard	Ratio error	Relative DCS error	Trans. error	Norm. error	Total error
30	1.6	3.0	4.1	5	6.0	9.5	3.0	13.8	15.6
40	2.0	2.5	2.5	5	4.1	7.6	3.0	14.9	16.2
50	2.3	2.5	1.8	5	4.0	7.5	3.0	14.3	15.6
54	1.8	2.5	2.0	0	6	6.6	3.0	10.5	11.1
100	1.8	2.5	1.7	9	5.4	11.1	3.0	12.1	15.5

FIG. 4. (a)–(e) Plots of $R_{H/He}$ values (Table I) determined from the present experiment ($\bigcirc$). For a discussion of errors see text, and for a summary of errors see Table III. In all cases, comparison with the results of the CCC (——), using Refs. [6] and [7], is made. The experimental $R_{H/He}$ of Ref. [12] at $E_0 = 100$ eV ($\triangle$) are also shown.

ment with the DWBA. In Fig. 5(d), at 54.4 eV, experimental He DCS's for the $n=2$ levels were not available. In consequence we have normalized our $R_{H/He}$ values to the CCC for He, as discussed earlier. We note very good agreement with the CCC at small θ, but this agreement gets worse as θ in-

creases, falling lower by as much as 40% at $\theta \approx 120°$. The lower values of our results possibly indicate that the CCC DCS's for He ($n=2$) may be low at large θ, a fact which is illustrated in Fig. 2, where it is compared to experiments [see especially Fig. 2(c), $E_0 = 50$ eV]. From this observation, we

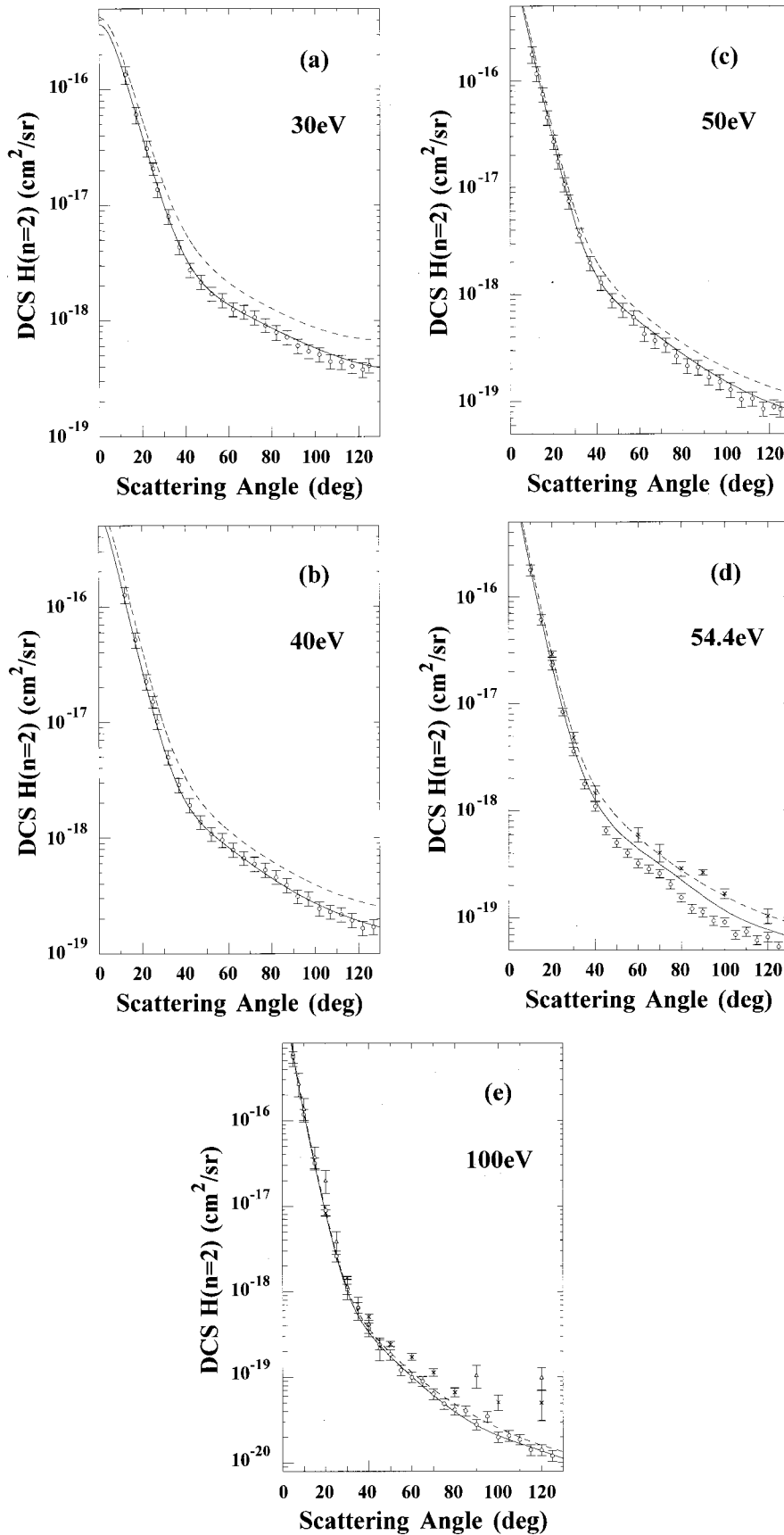FIG. 5. (a)–(e) Absolute electron impact DCS's for excitation of the $H(1\ ^2S) \rightarrow H(2\ ^2S + 2\ ^2P)$ transitions determined from this work ($\bigcirc$) compared to the present CCC (——) [6] and DWBA (---) [26]. At $E_0 = 54.4$ and 100 eV the experimental DCS's of Ref. [11] ($\times$) and [12] ($\triangle$) are also shown. See text for discussion. Note: The 54.4 eV DCS's are obtained via calibration with a theoretical standard [7]. See text for discussion.

infer that the CCC may possibly not have converged for electron-He DCS's as it has for H. We also observe that the absolute DCS's of Williams and Willis [11] are in disagreement with the CCC, but in excellent agreement with the DWBA. At $E_0 = 100$ eV, where we have calibrated our data to experimental He DCS's (as at $E_0 = 30$, 40, and 50 eV), we observe excellent agreement between the present DCS's and the CCC. We observe χ_ν^2 values of 0.61 with the CCC and 1.14 for the DWBA. However, even at this level of closeness, we can still discriminate between the better agreement of the CCC and the DWBA with the present DCS's. We note that at small θ, the DWBA and the CCC are in excellent agreement with each other, within 10% uncertainty. Comparison with the available DCS measurements of Williams and Willis [11] and Doering and Vaughan [12] at 100 eV shows that their DCS level at large scattering angles and apart from being sparse fall in disagreement with both theories. The DCS's measurements of Doering and Vaughan [12] rise considerably more steeply at the large scattering angles, and disagree with both the Williams and Willis [11] and the present values by as much as an order of magnitude. The small-angle DCS's of Doering and Vaughan [12] are, however, in good agreement with the present measurements.

VI. CONCLUSIONS

In conclusion, using a high intensity and stable source of H, we have measured accurate relative DCS's for electron impact excitation of the H($2\,^2S + 2\,^2P$) level from the ground state. Our experiment uses the method of mixtures with the calibration of our H ($n=2$) scattered electron intensities using available inelastic DCS standards in He. The DCS's results have error bars which average 7.5–11 % (relative) and 15.5–16 % (absolute) and show that the CCC theory is very accurate for the electron-H scattering problem. Our results support the electron-photon coincidence measurements of the Newcastle group [1], which (similarly to our DCS's) are in better agreement with the CCC [6] than the DWBA [26], but do not support those of the Maynooth group [8], which are (instead) in better agreement with the DWBA [26] results than the CCC [6]. However, this observation is limited since we measure DCS's and not coherence and correlation parameters.

The present measurements are useful in the following ways.

(i) They open up possibilities for measuring accurate inelastic (and possibly elastic) DCS's using the CCC H ($n=2$) as a calibration standard. We are considering implementing this method to measure absolute DCS's for other atomic (e.g., Ne and Ar) and dissociatable molecular targets (e.g., N_2, CO, O_2, and H_2O). The molecular targets will be mixed with the H atoms in a baffled post-discharge region before exiting the gas needle. The H calibration standard will be especially useful at values below $E_0 = 21$ eV, where He inelastic standards cannot be applied. We are also considering schemes by which absolute DCS's could be determined using this method in conjunction with the relative flow technique [29], but without the restriction of knowing the gas beam profiles. This should open possibilities for making reliable and accurate inelastic DCS's.

(ii) This work also indicates that the CCC may not have converged for electron-He scattering. Our experiments show that there are major disagreements between the CCC for He and existing experimental DCS's at $\theta > 60°$. Comparison between the CCC [6,7] with our $R_{H/He}$ values as well as with existing experimental absolute He ($n=2$) DCS's shows that the CCC may not have converged for He at large scattering angles. Very recently (during the writing of this paper), Cubric *et al.* [30] pointed out this large-angle disagreement between the CCC and experiments in He for He($2\,^3S, 2\,^1S, 2\,^3P$), although these measurements were normalized to the He($2\,^1P$) DCS's from the CCC itself. Such observations suggest that a detailed study of precision relative or absolute He DCS's will be very useful in pointing out where the CCC theory may need to be refined for He as a calibration DCS standard. This investigation is currently ongoing in our laboratory.

[1] H. A. Yalim, D. Cvejanovic, and A. Crowe, Phys. Rev. Lett. **79**, 2951 (1997).

[2] A. Zecca, G. P. Karwasz, and R. S. Brusa, Riv. Nuovo Cimento **19**, Series 1, No 3, 129 (1996).

[3] D. M. Crowe, X. Q. Guo, M. S. Lubell, J. Slevin, and M. Eminyan, J. Phys. B **23**, L325 (1990).

[4] M. A. Khakoo, D. Roundy, and F. Rugamas, Phys. Rev. Lett. **75**, 41 (1995).

[5] B. P. Donnelly, D. T. McLaughlin, and A. Crowe, J. Phys. B **27**, 319 (1990).

[6] I. Bray and A. Stelbovics, Phys. Rev. A **46**, 6995 (1992).

[7] D. V. Fursa and I. Bray, Phys. Rev. A **52**, 1279 (1995).

[8] R. W. O'Neill, P. J. M. van der Burgt, D. Dziczek, P. Bowe, S. Chwirot, and J. A. Slevin, Phys. Rev. Lett. **80**, 1630 (1998).

[9] A. Crowe (private communication).

[10] L. B. Madsen and K. Taulbjerg, Phys. Rev. A **52**, 2429 (1995).

[11] J. Williams and B. A. Willis, J. Phys. B **10**, 1641 (1975).

[12] J. P. Doering and S. O. Vaughan, J. Geophys. Res. **91**, 3279 (1986).

[13] J. F. Williams, J. Phys. B **8**, 2191 (1975).

[14] T. Shyn and A. Grafe, Phys. Rev. A **46**, 2949 (1992).

[15] M. A. Khakoo, M. Larsen, B. P. Paolini, X. Guo, I. Bray, A.

Stelbovics, I. Kanik, and S. Trajmar, Phys. Rev. Lett. **82**, 3980 (1999).

[16] M. A. Khakoo, D. Roundy, and F. Rugamas, Phys. Rev. A **54**, 4004 (1996).

[17] J. H. Brunt, G. C. King, and F. H. Read, J. Phys. B **10**, 1289 (1977).

[18] B. Paolini and M. A. Khakoo, Rev. Sci. Instrum. **69**, 3121 (1998).

[19] M. A. Khakoo, C. E. Beckmann, S. Trajmar, and G. Csanak, J. Phys. B **27**, 3159 (1994).

[20] Model 203, Variable Leak Valve, Granville-Phillips Company, 675 Arapahoe Avenue, Boulder, CO 80303-1398.

[21] N. Chan, D. M. Crowe, M. S. Lubell, F. C. Tang, A. Vasilakis, F. J. Mulligan, and J. Slevin, Z. Phys. D **10**, 893 (1988).

[22] J. Roder, H. Ehrhardt, I. Bray, and Dmitry V. Fursa, J. Phys. B **29**, L421 (1996).

[23] R. I. Hall, G. Joyez, J. Mazeau, J. Reinhardt, and C. Schermann, J. Phys. (Paris) **34**, 827 (1973).

[24] D. C. Cartwright, G. Csanak, S. Trajmar, and D. F. Register, Phys. Rev. A **45**, 1602 (1992).

[25] S. Trajmar, D. F. Register, D. C. Cartwright, and G. Csanak, J. Phys. B **25**, 4889 (1992).

[26] D. Madison, I. Bray, and I. E. McCarthy, J. Phys. B **24**, 3861 (1991); D. Madison (private communication).

[27] D. F. Register, S. Trajmar, and S. K. Srivatava, Phys. Rev. A **21**, 1134 (1980).

[28] Y. D. Wang, J. Callaway, and R. Unnikrishnan, Phys. Rev. A **49**, 1854 (1994).

[29] J. Nickel, P. Zetner, G. Shen, and S. Trajmar, J. Phys. B **22**, 730 (1989).

[30] D. Cubric, D. J. L. Mercer, J. M. Channing, G. C. King, and F. H. Read, J. Phys. B **32**, L45 (1999).